The Astrophysical Journal, 696:L129–L132, 2009 May 10 doi:10.1088/0004-637X/696/2/L129

THE COSMIC DECLINE IN THE H_2/H I RATIO IN GALAXIES

D. Obreschkow and S. Rawlings
Astrophysics, Department of Physics, University of Oxford, Keble Road, Oxford, OX1 3RH, UK
Received 2009 February 6; accepted 2009 April 1; published 2009 April 17

ABSTRACT

We use a pressure-based model for splitting cold hydrogen into its atomic (H I) and molecular (H_2) components to tackle the co-evolution of H I, H_2, and star formation rates (SFR) in $\sim 3 \times 10^7$ simulated galaxies in the Millennium simulation. The main prediction is that galaxies contained similar amounts of H I at redshift $z \approx 1$–5 than today, but substantially more H_2, in quantitative agreement with the strong molecular line emission already detected in a few high-redshift galaxies and approximately consistent with inferences from studies of the damped Lyman-α absorbers seen in the spectra of quasars. The cosmic H_2/H I ratio is predicted to evolve monotonically as $\Omega_{H_2}/\Omega_{HI} \propto (1+z)^{1.6}$. This decline of the H_2/H I ratio as a function of cosmic time is driven by the growth of galactic disks and the progressive reduction of the mean cold gas pressure. Finally, a comparison between the evolutions of H I, H_2, and SFRs reveals two distinct cosmic epochs of star formation: an early epoch ($z \gtrsim 3$), driven by the evolution of $\Omega_{HI+H_2}(z)$, and a late epoch ($z \lesssim 3$), driven by the evolution of $\Omega_{H_2}(z)/\Omega_{HI}(z)$.

Key words: cosmology: theory – galaxies: evolution – galaxies: high-redshift – ISM: atoms – ISM: molecules

1. INTRODUCTION AND KEY IDEA

Neutral hydrogen is the fuel for the formation of stars. The cosmic star formation rate (SFR) density as inferred from ultraviolet, far-infrared, and submillimeter observations increases by an order of magnitude from redshift $z = 0$ to $z = 2$ (Hopkins 2007). Hence neutral hydrogen in early galaxies was either more abundant or transformed into stars more efficiently than today.

A useful quantity in this context is the star formation efficiency (SFE) of a galaxy, defined as the SFR divided by the gas mass. The weak cosmic evolution of the density of neutral atomic hydrogen (H I), derived from Lyman-alpha absorption against distant quasars (Lah et al. 2007; Pontzen & Pettini 2009), indicates a strongly increased SFE at high z. But recent detections of strong molecular line emission in ordinary galaxies at $z = 1.5$ (Daddi et al. 2008) suggest that the SFEs of these galaxies are similar to those seen today. The seeming contradiction between these two conclusions arises from the conceptual confusion of SFEs inferred from galactic H I with those inferred from H_2. In fact, it is crucial to distinguish between the two quantities $\mathrm{SFE_{HI}} \equiv \mathrm{SFR}/M_{HI}$ and $\mathrm{SFE_{H_2}} \equiv \mathrm{SFR}/M_{H_2}$. In principle, there is no contradiction between the detected strong cosmic evolution of $\mathrm{SFE_{HI}}$ and the weak evolution of $\mathrm{SFE_{H_2}}$—these empirical findings could simply imply that the H_2/H I mass ratios R_{mol}^{galaxy} of galaxies increase substantially with z.

In this Letter, we show that there is indeed strong theoretical support for such an increase of R_{mol}^{galaxy} with z in regular galaxies. This evolution is driven by the approximate scaling of galaxy sizes as $(1+z)^{-1}$ predicted by dark matter theory (Gunn & Gott 1972) and confirmed by observations in the Ultra Deep Field (Bouwens et al. 2004). Hence the cold gas disks at high redshift must, on average, be denser than today. Combining this prediction with the relation between gas pressure and H_2/H I ratios in nearby galaxies (e.g., Blitz & Rosolowsky 2006) leads to the conclusion that R_{mol}^{galaxy} must increase dramatically with z. Our quantitative predictions of this evolution rely on a recently presented semianalytic numerical simulation of H I and H_2 in $\sim 3 \times 10^7$ simulated galaxies (Obreschkow et al. 2009), based on the Millennium simulation (Springel et al. 2005).

Section 2 overviews our simulation method and the model for the H_2/H I ratio in galaxies. In Section 3 we present and interpret the predicted evolution of galactic H I and H_2 and their relation to star formation. Section 4 compares these predictions to empirical data, and Section 5 summarizes our key conclusions.

2. SIMULATING H I AND H_2 IN GALAXIES

2.1. Physical Model for Galactic H_2/H I Ratios

In virtually all regular galaxies in the local universe, whether spirals (e.g., Leroy et al. 2008) or ellipticals (e.g., Young 2002), the cold gas resides in a flat disk. Some observations of CO at $z \approx 2$ (Tacconi et al. 2006) suggest that even at high redshift most cold gas lies in disks. Based on this evidence, we have recently introduced a model for the distributions of H I and H_2 in regular galaxies (Obreschkow et al. 2009), assuming that all cold gas resides in a flat symmetric disk with an exponential surface density profile and that the local H_2/H I ratio is dictated by the kinematic gas pressure (Blitz & Rosolowsky 2006; Leroy et al. 2008). Within these assumptions, we could show that the H_2/H I mass ratio R_{mol}^{galaxy} of an entire galaxy is given by

$$R_{mol}^{galaxy} = \left(3.44\, {R_{mol}^{c}}^{-0.506} + 4.82\, {R_{mol}^{c}}^{-1.054}\right)^{-1}, \qquad (1)$$

where R_{mol}^{c} represents the H_2/H I ratio at the galaxy center. R_{mol}^{c} can be approximated as

$$R_{mol}^{c} = \left[11.3\ \mathrm{m^4\ kg^{-2}}\, r_{disk}^{-4} M_g \left(M_g + 0.4\, M_s^{disk}\right)\right]^{0.8}, \qquad (2)$$

where r_{disk} is the exponential scale radius of the disk, M_g is the total cold gas mass, and M_s^{disk} is the stellar mass in the disk. Equations (1), (2) constitute a physical model to estimate R_{mol}^{galaxy} in regular galaxies based on M_s^{disk}, M_g, and r_{disk}. In order to predict the cosmic evolution of R_{mol}^{galaxy}, we therefore require a model for the co-evolution of M_s^{disk}, M_g, and r_{disk} in galaxies. To this end, we adopted the virtual galaxy catalog of the Millennium simulation described in Section 2.2. The limitations of the model

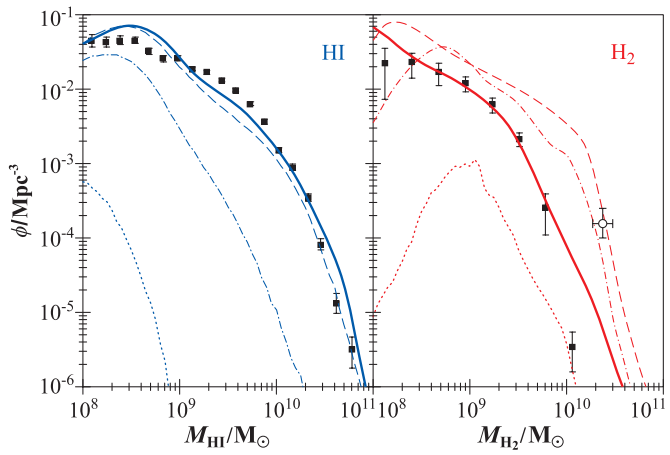

Figure 1. MFs of H I and H_2. Lines show the simulation results at $z = 0$ (solid), $z = 2$ (dashed), $z = 5$ (dash-dotted), $z = 10$ (dotted). Square dots represent the empirical data and 1-σ scatter at $z = 0$ (Zwaan et al. 2005a; Obreschkow & Rawlings 2009b), and the open circle represents our density estimate at $z = 1.5$ (Section 4) based on Daddi et al. (2008).

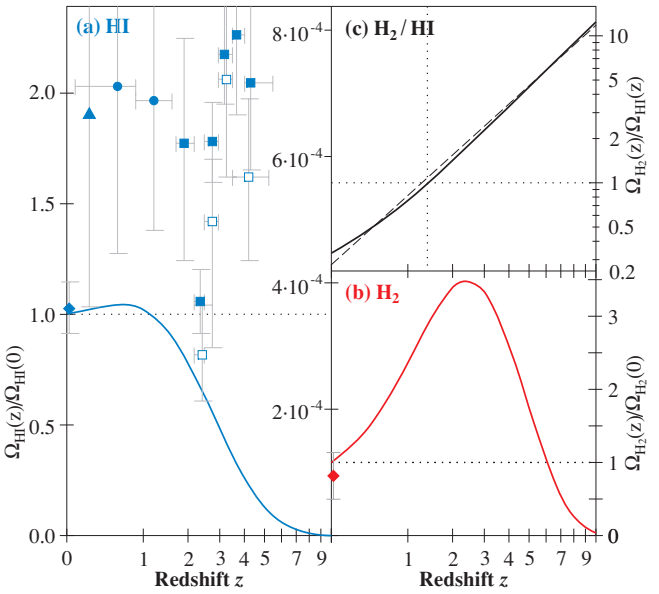

Figure 2. Evolution of the fractional densities of H I and H_2. Solid lines represent the simulation results and the dashed line is the power-law fit of Equation (3). The points represent observations described in Section 4.

of Equations (1), (2) and their impact on the predicted H_2/H I ratios are discussed in Obreschkow et al. (2009).

2.2. H I and H_2 in the Millennium Simulation

The Millennium simulation (Springel et al. 2005) is an N-body simulation within the ΛCDM cosmology of $\sim 10^{10}$ gravitationally interacting particles in a periodic box of comoving volume $(500/h\ \mathrm{Mpc})^3$, where $H_0 = 100\,h$ km s^{-1} Mpc^{-1} and $h = 0.73$. The evolving large-scale structure generated by this simulation served as the skeleton for the simulation of $\sim 3 \times 10^7$ galaxies at the halo centers. In the "semianalytic" approach adopted by De Lucia & Blaizot (2007), galaxies were considered as simplistic objects with a few global properties that are evolved stepwisely using a list of physical prescriptions. For example, the total amount of cold hydrogen (H I+H_2) in a galaxy is defined by the history of the net accretion, which in the model consists of (1) the infall of gas from the hot halo, (2) the loss of gas by star formation, and (3) outflows driven by supernovae and active galactic nuclei. Star formation in each galaxy is tackled using a law, where all cold gas above a critical surface density is transformed into stars on a timescale proportional to the dynamical time of the disk (for details, see Croton et al. 2006).

In Obreschkow et al. (2009), we applied the model of Section 2.1 to the simulated galaxies in the catalog of De Lucia & Blaizot (2007) ("DeLucia catalog") to split their cold hydrogen masses into H I and H_2. Our simulation successfully reproduced many local observations of H I and H_2, such as mass functions (MFs), mass–diameter relations, and mass–velocity relations. Yet, the high-redshift predictions are inevitably limited by the semianalytic recipes of the DeLucia catalog. The most uncertain recipes are those related to mergers (e.g., feedback of black hole coalescence and starbursts), but they have a minor effect on the cosmic space densities of H I and H_2, since most cold gas in the simulation is found in regular disk galaxies[1] with at most minor merger histories. However, inaccurate prescriptions for isolated galaxies could significantly affect the space densities of H I and H_2, and it may well become necessary to refine our simulation as improved semianalytic methods come on line.

[1] In contrast, a significant fraction of the *stars* at $z = 0$ is in massive elliptical galaxies with violent merger histories, but even those galaxies formed most stars in their spiral progenitors.

3. RESULTS

3.1. Predicted Evolution of H I and H_2

Figure 1 shows the predicted evolution of the H I–MF and H_2–MF, i.e., the comoving space densities of sources per logarithmic mass interval. The predictions at $z = 0$ roughly agree with available observational data, but the obvious differences, such as the spurious bumps around $M_{\rm HI} \approx 10^{8.5}$ and $M_{\rm H_2} \approx 10^8$ (a mass resolution limit), have been discussed in Obreschkow et al. (2009).

The predicted H I masses remain roughly constant from $z = 0$ to $z = 2$, while H_2 masses increase dramatically. These different evolutions are also reflected in the comoving space densities $\Omega_{\rm HI} \equiv \rho_{\rm HI}/\rho_{\rm c}$ and $\Omega_{\rm H_2} \equiv \rho_{\rm H_2}/\rho_{\rm c}$, where $\rho_{\rm c}(z) = 3H^2(z)/(8\pi G)$ is the critical density for closure. Here, $\Omega_{\rm HI}$ and $\Omega_{\rm H_2}$ only account for gas in galaxies, excluding unbound H I between the first galaxies (Becker et al. 2001) or possible H_2 in halos (Pfenniger & Combes 1994). The simulated functions $\Omega_{\rm HI}(z)$ and $\Omega_{\rm H_2}(z)$ are shown in Figures 2(a), (b), while Figure 2(c) represents their ratio $R_{\rm mol}^{\rm cosmic}(z) \equiv \Omega_{\rm H_2}(z)/\Omega_{\rm HI}(z)$, which is closely described by the power law

$$R_{\rm mol}^{\rm cosmic}(z) \approx 0.3 \times (1+z)^{1.6}. \quad (3)$$

The simulation yields $R_{\rm mol}^{\rm cosmic}(0) \approx 0.3$ and finds the crossover, $R_{\rm mol}^{\rm cosmic}(z) = 1$, at $z \approx 1.4$. Our model predicts that Equation (3) extends to epochs, where the first galaxies formed, but this prediction is likely to breakdown at the highest redshifts, where the formation of H_2 was inhibited by the lack of metals (Abel & Haiman 2000).

Physically, the strong evolution of H_2/H I is essentially driven by the size evolution of galaxies and their halos. The Millennium simulation assumes that the virial radius $r_{\rm vir}$ of a spherical halo always encloses a mass with an average density 200 times above the critical density $\rho_{\rm c} \propto H^2$ (Croton et al. 2006). Hence, for a fixed halo mass, $r_{\rm vir} \propto H^{-2/3}$. In a flat universe this implies

$$r_{\rm vir} \propto \left[\Omega_{\rm m}(1+z)^3 + \Omega_\Lambda\right]^{-1/3}, \quad (4)$$

which asymptotically tends to $r_{\rm vir} \propto (1+z)^{-1}$ for high z. By virtue of the theory of Fall & Efstathiou (1980), this cosmic scaling of $r_{\rm vir}$ results in a similar scaling of the disk radius, i.e., $r_{\rm disk} \propto (1+z)^{-1}$, consistent with observations in the Ultra Deep Field (Bouwens et al. 2004).

For the gas-dominated galaxies in the early universe, Equation (2) reduces to $R^{\rm c}_{\rm mol} \propto r_{\rm disk}^{-3.2} M_{\rm g}^{1.6}$. Yet, the cold gas masses $M_{\rm g}$ of individual galaxies in the simulation evolve weakly with cosmic time due to a self-regulated equilibrium between the net inflow of gas and star formation. In fact, most of the evolution of $\Omega_{\rm HI+H_2}$ in the redshift range $z \approx 3$–10 is due to the build-up of new galaxies. Therefore, $R^{\rm c}_{\rm mol} \propto r_{\rm disk}^{-3.2} \propto (1+z)^{3.2}$. At redshifts $z \approx$ 1–10, $R^{\rm c}_{\rm mol}$ typically takes values between 10 and 10^4, such that Equation (1) can be approximated as $R^{\rm galaxy}_{\rm mol} \propto {R^{\rm c}_{\rm mol}}^{0.5}$. Hence $R^{\rm galaxy}_{\rm mol} \propto (1+z)^{1.6}$, which explains the scaling of Equation (3).

The cosmic evolution of $\Omega_{\rm H_2}$ shown in Figure 2 can be divided in two epochs: the *early epoch* ($z \gtrsim 3$), where $\Omega_{\rm H_2}$ increases with cosmic time, and the *late epoch* ($z \lesssim 3$), where $\Omega_{\rm H_2}$ decreases with time. In the early epoch, $R^{\rm galaxy}_{\rm mol} > 1$ implies $\Omega_{\rm H_2} \approx \Omega_{\rm HI+H_2}$, and hence the growth of $\Omega_{\rm H_2}$ reflects the general increase of $\Omega_{\rm HI+H_2}$ due to the intense assembly of new galaxies. In the late epoch, $R^{\rm galaxy}_{\rm mol} \lesssim 1$ implies that $\Omega_{\rm H_2} \approx R^{\rm cosmic}_{\rm mol} \Omega_{\rm HI+H_2}$. At this epoch the formation of the massive galaxies in the simulation is completed, i.e., $\Omega_{\rm HI+H_2}(z) \approx$ const and $\Omega_{\rm H_2} \propto R^{\rm cosmic}_{\rm mol}$. Thus the decrease of $\Omega_{\rm H_2}$ in this late epoch is driven by cosmic decline in $R^{\rm cosmic}_{\rm mol}$ or, physically, by the cosmic evolution of pressure.

3.2. Link Between H I, H_2, and Star Formation

To discuss the global cosmic evolution of the efficiencies $\rm SFE_{HI}$ and $\rm SFE_{H_2}$ (Section 1), we shall define

$$\langle {\rm SFE_{HI}} \rangle \equiv \rho_{\rm SFR}/\rho_{\rm HI}\,, \quad \langle {\rm SFE_{H_2}} \rangle \equiv \rho_{\rm SFR}/\rho_{\rm H_2}, \qquad (5)$$

where $\rho_{\rm HI} \propto \Omega_{\rm HI}$, $\rho_{\rm H_2} \propto \Omega_{\rm H_2}$, and $\rho_{\rm SFR}$ denote the comoving space densities of H I, H_2, and SFR.

In the semianalytic recipes of the DeLucia catalog, SFRs are estimated from the gas density and the dynamical timescale of the disk (Section 2.2). This Schmidt–Kennicutt law (Schmidt 1959; Kennicutt 1998) for star formation makes similar predictions to models based on cold gas pressure (e.g., Blitz & Rosolowsky 2006), and therefore the SFRs in the DeLuica catalog are, by default, approximately consistent with our model to split cold hydrogen into H I and H_2. The evolutions of $\langle {\rm SFE_{HI}} \rangle$ and $\langle {\rm SFE_{H_2}} \rangle$ predicted by the simulation again reflect the marked difference between H I and H_2. They are approximated (∼20% relative error) by the power laws,

$$\langle {\rm SFE_{HI}} \rangle \big/ \left[{\rm Gyr}^{-1}\right] = 0.23\,(1+z)^{2.2}, \qquad (6)$$

$$\langle {\rm SFE_{H_2}} \rangle \big/ \left[{\rm Gyr}^{-1}\right] = 0.75\,(1+z)^{0.6}, \qquad (7)$$

out to $z \approx 8$.

Due to the low power in Equation (7) $\rho_{\rm SFR}(z)$ is approximately proportional to $\Omega_{\rm H_2}(z)$. We can therefore apply the two cosmic epochs of $\Omega_{\rm H_2}(z)$ introduced in Section 3.1 to the history of star formation: In the *early epoch* ($z \gtrsim 3$), $\rho_{\rm SFR}$ increases with cosmic time, proportionally to $\Omega_{\rm HI+H_2}$. This increase traces the dramatic assembly of new galaxies. In the *late epoch* ($z \lesssim 3$), $\rho_{\rm SFR}$ decreases roughly proportionally to $\Omega_{\rm H_2}/\Omega_{\rm HI}$. This epoch is driven by the cosmic evolution of pressure (or density) in galactic disks. This interpretation of the history of star formation does not, in fact, conflict with the picture that star formation is ultimately defined by the accreted cold gas mass (see Section 2.2) and a Schmidt–Kennicutt-type law for transforming this gas into stars. Our H_2/H I-based interpretation simply adds another layer to the causal chain, by suggesting that cold gas mass and density ultimately dictate the amount of molecular material available for star formation.

The simulation also includes star formation via merger-driven starbursts, associated with the creation of the stellar spheroids of early-type spiral or elliptical galaxies. However, the cosmic star formation density caused by this process only accounts for about 1% of $\rho_{\rm SFR}$, because even elliptical galaxies in the simulation formed most of their stars in their spiral progenitors.

4. COMPARISON WITH OBSERVATIONS

The DeLucia catalog and our post-processing to assign H I and H_2, rely on established data of the local universe. Our simulated H I and H_2 properties at $z = 0$ are consistent with all available observations, i.e., MFs (see Figure 1), disk sizes, and velocity profiles (Obreschkow et al. 2009). In particular, the simulated values $\Omega_{\rm HI}(0) = 3.5 \times 10^{-4}$ and $\Omega_{\rm H_2}(0) = 1.2 \times 10^{-4}$ are consistent with the values (diamonds in Figure 2) derived from the MFs observed in H I and CO emission at $z \approx 0$ (Zwaan et al. 2005a; Obreschkow & Rawlings 2009b). At $z > 0$, the currently available data is sparse, especially in emission.

The only measurement of $\Omega_{\rm HI}$ in emission at intermediate redshift is based on the stacking of 121 galaxies at $z = 0.24$ (Lah et al. 2007; triangle in Figure 2). The detection is speculative (see Figure 7 in Lah et al. 2007), but roughly consistent with our simulation. All other measurements of $\Omega_{\rm HI}$ at $z > 0$ rely on absorption detections of damped Lyman-α systems (DLAs). Respective data points from Rao et al. (2006) (circles in Figure 2) and Prochaska et al. (2005) (filled squares) are, taken together, inconsistent with the predicted values of $\Omega_{\rm HI}$. In contrast, Zwaan et al. (2005b) demonstrated that the population of H I galaxies in the local universe can fully explain the column density distributions of DLAs out to $z = 1.5$, consistent with the nearly absent evolution of $\Omega_{\rm HI}$ from $z = 0$ to $z = 1.5$ predicted by our simulation. At present it is therefore difficult to judge whether the simulation is inconsistent with empirical data at these low redshifts covering 2/3 of the age of the universe. At higher redshifts, however, the measurements of $\Omega_{\rm HI}$ seem not conceivable with the simulated result, and even accounting for gravitational lensing by the DLAs only corrects the empirical values of $\Omega_{\rm HI}$ by about 30% (open squares in Figure 2; Prochaska et al. 2005). The simulated values of $\Omega_{\rm HI}$ are likely to underestimate the real values by about a factor 2—a plausible offset given the long list of simplifying approximations required from the *N*-body Millennium simulation to our final post-processing of hydrogen in galaxies. Much progress could be expected from treating H I masses and H_2 masses as separate quantities directly in the semianalytic galaxy simulation. This would allow, for example, to refine the feedback mechanisms for suppression of gas infall (explained in Croton et al. 2006), such that H I can still be accreted, while the formation of H_2 and stars is inhibited. Such a semianalytic setting would also allow to implement a recipe for the large-scale dissociation of molecular gas by the radiation of newly formed stars (Allen et al. 1986). Both examples would effectively increase the amount of H I in high-redshift galaxies.

The most representative high-redshift observations of molecular gas to date rely on two galaxies (*BzK*-4171 and *BzK*-21000)

at $z \approx 1.5$, reliably detected in CO(2–1) emission by Daddi et al. (2008). Unlike other CO sources at similar or higher z, these objects are ordinary massive galaxies with FIR luminosities of $L_{\rm FIR} \approx 10^{12}\,L_\odot$, selected only due to the availability of precise spectroscopic redshifts. From these two detections, we estimated the H_2-space density (empty circle in Figure 1) as follows: The mass interval spans between the masses $M_{\rm H_2} \approx 2 \times 10^{10}\,M_\odot$ and $M_{\rm H_2} \approx 3 \times 10^{10}$, respectively obtained for *BzK*-4171 and *BzK*-21000 by applying the CO-to-H_2 conversion of $\alpha = 1\,M_\odot({\rm K\ km\ s^{-1}\ pc^{-2}})^{-1}$ (Daddi et al. 2008). The space density of these CO sources was approximated as the space density of FIR sources at $L_{\rm FIR} \approx 10^{12}\,L_\odot$, based on the fact that all (both) targeted galaxies with $L_{\rm FIR} \approx 10^{12}\,L_\odot$ revealed similar CO-luminosities $L_{\rm CO}$. We estimate their space density to be between $1\text{–}2 \times 10^{-4}\ {\rm Mpc^{-3}}$ per unit of $\log(L_{\rm FIR})$, by extrapolating the FIR luminosity functions of Huynh et al. (2007). Since $L_{\rm FIR} \propto L_{\rm CO} \propto M_{\rm H_2}$, we find roughly the same space density per unit $\log(M_{\rm H_2})$. These result is consistent with the simulated H_2–MF at $z = 2$ (Figure 1).

Considering H_2-absorption studies, Curran et al. (2004) and Noterdaeme et al. (2008) have determined H_2/H I ratios in DLAs that showed H_2-absorption. They found H_2/H I ratios of $\sim 10^{-6}$ to $\sim 10^{-2}$ at $z \approx 2\text{–}3$, clearly much smaller than our prediction for $\Omega_{\rm H_2}/\Omega_{\rm HI}$. We argue that measurements of H_2/H I in DLAs do not trace $\Omega_{\rm H_2}/\Omega_{\rm HI}$ since DLAs are by definition H I-selected objects and H_2 has a much smaller space coverage than H I. In fact, H_2 disks in galaxies are much smaller than H I disks, especially at high z (Obreschkow & Rawlings 2009a), and even inside the H_2 disks the coverage of H_2 is small compared to H I (e.g., Ferrière 2001). A more detailed explanation of why H_2-searches in DLAs are expected to be difficult was given by Zwaan & Prochaska (2006) based on the analysis of CO-emission maps of local galaxies.

5. CONCLUSIONS

In this Letter, we have predicted the cosmic evolution of H I and H_2 masses in $\sim 3 \times 10^7$ simulated galaxies based on the Millennium simulation. The predicted cosmic decline in the H_2/H I ratio is consistent with the weak cosmic evolution of $\Omega_{\rm HI}$ inferred from DLA-studies and recent observations revealing a significantly enhanced space density of H_2 at $z = 1.5$ (Daddi et al. 2008).

Perhaps the most important conclusion is that H I and H_2 masses evolve very differently with cosmic time and therefore cannot be used as proportional tracers of one another, especially not for the purpose of high-redshift predictions. There is no contradiction between the large H_2 masses detected at high z, which imply values of $\rm SFE_{H_2}$ similar to those in the local universe, and the weak evolution of H I, implying massively increased values of $\rm SFE_{HI}$ at high z.

This work is supported by the European Community Framework Programme 6, Square Kilometre Array Design Studies (SKADS), contract no 011938. The Millennium Simulation databases and the web application providing online access to them were constructed as part of the German Astrophysical Virtual Observatory.

REFERENCES

Abel, T., & Haiman, Z. 2000, in Molecular Hydrogen in Space, ed. F. Combes & G. Pineau Des Forets (Cambridge: Cambridge Univ. Press), 237
Allen, R. J., Atherton, P. D., & Tilanus, R. P. J. 1986, Nature, 319, 296
Becker, R. H., et al. 2001, AJ, 122, 2850
Blitz, L., & Rosolowsky, E. 2006, ApJ, 650, 933
Bouwens, R. J., Illingworth, G. D., Blakeslee, J. P., Broadhurst, T. J., & Franx, M. 2004, ApJ, 611, L1
Caputi, K. I., et al. 2007, ApJ, 660, 97
Croton, D. J., et al. 2006, MNRAS, 365, 11
Curran, S. J., Murphy, M. T., Pihlström, Y. M., Webb, J. K., Bolatto, A. D., & Bower, G. C. 2004, MNRAS, 352, 563
Daddi, E., Dannerbauer, H., Elbaz, D., Dickinson, M., Morrison, G., Stern, D., & Ravindranath, S. 2008, ApJ, 673, L21
De Lucia, G., & Blaizot, J. 2007, MNRAS, 375, 2
Fall, S. M., & Efstathiou, G. 1980, MNRAS, 193, 189
Ferrière, K. M. 2001, Rev. Mod. Phys., 73, 1031
Gunn, J. E., & Gott, J. R. I. 1972, ApJ, 176, 1
Hopkins, A. M. 2007, in ASP Conf. Ser. 380, Deepest Astronomical Surveys, ed. J. Afonso, H. C. Ferguson, B. Mobasher, & R. Norris (San Francisco, CA: ASP), 423
Huynh, M. T., Frayer, D. T., Mobasher, B., Dickinson, M., Chary, R.-R., & Morrison, G. 2007, ApJ, 667, L9
Kennicutt, R. C., Jr. 1998, ApJ, 498, 541
Lah, P., et al. 2007, MNRAS, 376, 1357
Leroy, A. K., Walter, F., Brinks, E., Bigiel, F., de Blok, W. J. G., Madore, B., & Thornley, M. D. 2008, AJ, 136, 2782
Noterdaeme, P., Ledoux, C., Petitjean, P., & Srianand, R. 2008, A&A, 481, 327
Obreschkow, D., Croton, D., De Lucia, G., Khochfar, S., & Rawlings, S. 2009, ApJ, submitted
Obreschkow, D., & Rawlings, S. 2009a, ApJL, submitted
Obreschkow, D., & Rawlings, S. 2009b, MNRAS, 394, 1857
Pfenniger, D., & Combes, F. 1994, in Particle Astrophysics, Atomic Physics and Gravitation, ed. J. Tran Thanh van, G. Fontaine, & E. Hinds (Gif-sur-Yvette: Editions Frontières), 107
Pontzen, A., & Pettini, M. 2009, MNRAS, 393, 557
Prochaska, J. X., Herbert-Fort, S., & Wolfe, A. M. 2005, ApJ, 635, 123
Rao, S. M., Turnshek, D. A., & Nestor, D. B. 2006, ApJ, 636, 610
Schmidt, M. 1959, ApJ, 129, 243
Springel, V., et al. 2005, Nature, 435, 629
Tacconi, L. J., et al. 2006, ApJ, 640, 228
Young, L. M. 2002, AJ, 124, 788
Zwaan, M. A., Meyer, M. J., Staveley-Smith, L., & Webster, R. L. 2005a, MNRAS, 359, L30
Zwaan, M. A., & Prochaska, J. X. 2006, ApJ, 643, 675
Zwaan, M. A., van der Hulst, J. M., Briggs, F. H., Verheijen, M. A. W., & Ryan-Weber, E. V. 2005b, MNRAS, 364, 1467